Nicodème Rouger

Experimental work

M2 TMA

2025 - 2026

Contents

Résumé

La turbulence reste de nos jours un problème ouvert. Dans ce cadre, les aspects numériques et expériementaux de cette discipline sont un enjeu majeur à la meilleure compréhension de la physique sous-jacente.

Ce rapport présente 4 travaux pratiques réalisés dans le cadre du master ”Turbulence: Méthodes et Applications” (TMA). Ces travaux présentent une large gamme de méthodes expérimentales et d'analyse du signal associés à la turbulence sous toutes ses formes. Cette dernière est mise en évidence aussi bien dans les ondes, les vents atmosphériques, les instabilités que dans les océans. Les mesures vont du micro sonore à la mesure optique (en ”Particle Image Velocimetry” - PIV - ou profilométrie) en passant par les anémomètres soniques et les tubes pitot. Les méthodes d'analyse du signal sont tout aussi variées: du simple spectre à une transformée de Fourier spatio-temporelle en utilisant au besoin des méthodes de moyennage telles que la méthode de Welch.

Les enjeux de ces traitements et méthodes sont présentés au travers d'expériences réalisées au Laboratoire des Écoulements Géophysiques et Industriels de Grenoble ainsi que dans la clairière de Frepeyret sur le site de Belledonne.

Abstract

Turbulence remains an open problem today. In this context, the numerical and experimental aspects of this discipline are key to a better understanding of the underlying physics.

This report presents four practical projects carried out as part of the Master ”Turbulence: Méthodes et Applications” (TMA). These projects cover a wide range of experimental methods and signal analysis techniques associated with turbulence in all its forms. Turbulence is highlighted in waves, atmospheric winds, instabilities and oceans. The measurements range from acoustic to optical (”Particle Image Velocimetry” - PIV - or profilometry), including sonic anemometers and Pitot tubes. Signal analysis methods are equally varied: from simple spectrum to spatio-temporal Fourier transform, using averaging methods such as the Welch method.

The challenges of these processes and methods are presented through experiments carried out at the Laboratoire des Écoulements Géophysiques et Industriels in Grenoble and in the Frepeyret clearing on the Belledonne site.

AI use

In this report, Artificial Intelligence has been used as a tool for developping and debuging some particular parts of data analysis programs. Some translations have been also performed with this technology. Under no circumstances this tool has been used to construct physical discussion or any type of text paragraph.

1 Introduction

The M2 TMA offers training with a strong experimental component. In this context, a serie of experimental work has been achieved. All studies are related to turbulence showing the diversity of this topic. Fieldwork or laboratory experiments, considering fluids or other mecanical support (like musical gong), performing a huge range of signal analysis, trubulence can be highlighted in many different ways.

The four subjects presented here show this diversity. Starting from wave turbulence showing how slightly non linear wave propagation can leads to turbulent properties. Continuing with the role of fluid turbulence and earth rotation in the formation of the Gulf Stream current. Then, considering a wake instability and showing the link with turbulence. Finishing with fieldwork measurements on the atmospheric boundary layer. All experiment exposed here give a part of the entire table of what is turbulence and how can it be studied and represented.

2 Theory

2.1 Signal processing

In most of the parts of this report measurements are done and saved numericaly. To do so, the signal must be discretised in space and time. It's done acording to the number of bites allowed for each measuremenent and to the sampling frequency. After this quantisation, the signal is just an array of integers that can be analaysed such as analog signal (taking care to limits like Shannon theorem).

Taking into account sensor properties, one can make a link between integer values of the numerical signal and the physical value of the analog one. In most of the figures of this report, physical quantities are represented in unit of the step of quantisation. When it's the case no physical unit is mentioned because the corresponding value is dimensionless. This convention is used when the absolute value of the signal is not necessary to understand the underlying physics.

2.2 Welch method

The Welch method is a way to reduce noise in a Fourier transform (in return the spectrum loses in resolution). This method calculate Fourier transform of a range of signals extracted from the original one. An average is then performed over all the resulting spectra. The range of signal is generated splinting up the whole signal into ovelapping segments and windowing them to reduce Gibbs phenomenon.

For example if the whole signal have n points, each segment have a given length m and each segment ovelap the previous one by d points, one can discuss some particular cases:

- **d=0:** there is no overlapping and the Welch method correspond to the Bartlett's method: averaging spectra on calculations performed over contiguous time windows assuming ergodicity. In this case average is performed over $\lfloor n/m \rfloor$ segments.
- $\mathbf{d = \frac{m}{2}}$**:** the overlapping is about 50% and the average is performed over $\left\lfloor \frac{n-m}{m-d} \right\rfloor + 1$ segments.

Generaly the second case mentioned is used to reduce noise in a spectrum. It allows to keep a good balance between spectrum resolution and noise reduction making sure signals are not too correlated. In fact, performing Welch method with an overlapping of 99% would amount to averaging strongly correlated signals which loose the pertinence of the averaging.

2.3 Fourier Transform Profilometry

This method, described in details in [3], allows to measure the deformation of thin elastic plate over space and time. A sine profile is projected on the surface and a camera capture the resulting image (see fig. 1). A deformation of the plate leads to a phase shift in the measured picture. At first order in deformation the phase shift is linear with deformation.

This setup allows to extract deformation and velocity of the plate from a video. These properties are calculated in every position captured by the camera with a resolution all the more precise as the camera is high-resolution.

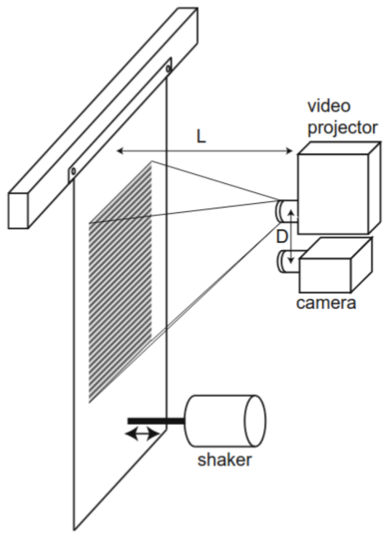

Figure 1: Profilometry principle on a square plate (figure from [4]).

2.4 Particle Image Velocimetry (PIV)

Particle Image Velocimetry (PIV) measure a fluid velocity in a plane by tracking the motion of tracer paticles with a camera. The plane considered must be illuminated by a laser sheet. To compute velocities, particles displacement are calculated between two successive images using cross-correlation. Time and space resolution are defined by the camera properties. To give pertinent measurements the tracer size must be small enough so they do not impact the fluid dynamic. In other terms the Stockes number must be much smaller than 1:

$$Stk = \frac{t_0 u_0}{l_0} \ll 1.$$

With t_0 the relaxation time of the particle, u_0 the fluid velocity of the flow well away from the particle and l_0 the characteristic dimension of the particle.

3 Vibrating plate: Gong

3.1 System considered

A metalic gong is studied. This gong is circular with a diameter around 50 cm. This vibrating plate is studied analysing the song emitted by it in a first part. In a second part optical measurements are done to analise space and time deformations of this system.

Goal: show that the energy propagate inside the plate under a wave form and highlight the presence of turbulence in these waves.

3.2 Acoustic measurements

Measurements are done with a microphone about 2 m away from the gong. Recording are performed with Audacity.

3.2.1 Steady state

Computing the Fourier transform of the acoustic signal emitted by the gong in a steady state is a good way to prove that waves are propagating in the system. In fact, a finite system in wich waves are propagating oscillate at discrete and well defined frequencies. Indeed, if waves

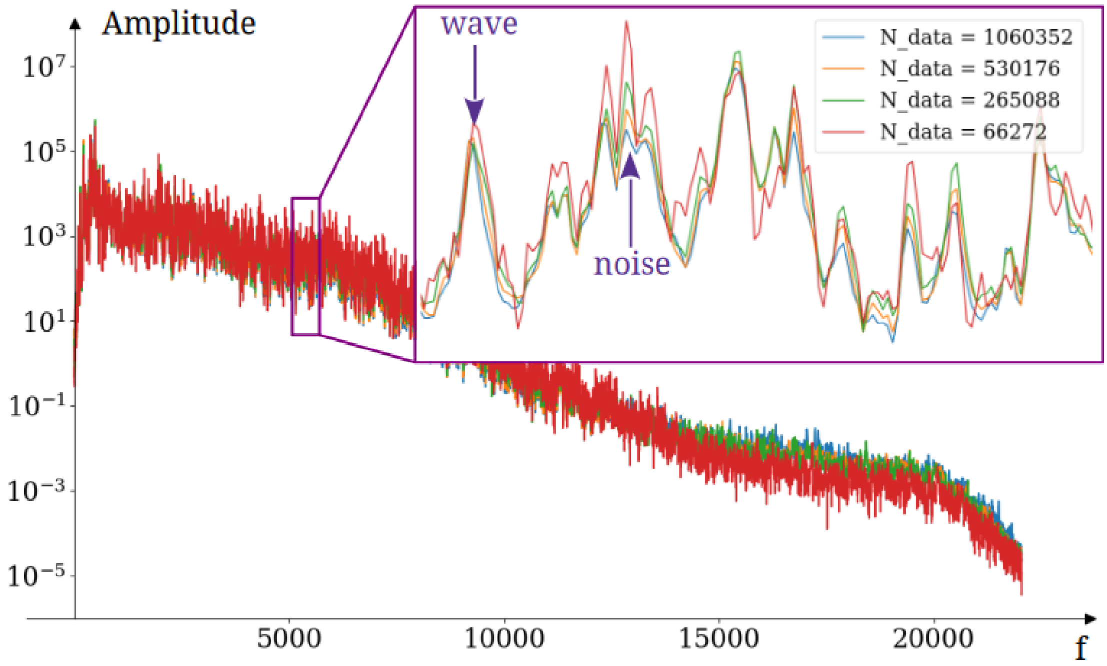

Figure 2: Spectrum of the steady state sound signal. The zoom shows that some peaks amplitude are decrasing while increasing the Welch meaning (noise peaks) and some others peaks amplitude remain constant for each Welch meaning (wave peaks).

are propagating in the gong, the Fourier transform of the sound emitted by it must show sharp peaks (each peak corresponding to a vibrating mode of the plate).

To put the system in a steady state blows are struck by hand the most regularly possible. The recording is started when the song seems to be steady. Measurements are done with 3 different forcing intensities.

Fourier transform are then performed on recorded signals. Unfortunately, the resulting spectra are too noisy to show well defined peaks that would be caracteristic of a wave propagation. To reduce noise the Welch method is applied (see §2.2).

To show that waves are propagating inside the gong, special attention must be paid to the way the Welch method is applied. In fact, two fenomena are superposing and interfering here:

- reduction of the amplitude of the noise allowed by increasing the number of segments on wich averaging is performed,
- reduction of the frequency resolution (when the number of points per segment decrase) that implies reduction of the amplitude of the physical peaks that are pursued (reduction of the frequency resolution means averaging the spectra between two consecutive frequencies so the amplitude of the sharp peaks diminishes).

To have identical resolution in frequency while reducing noise in the spectrum, Welch method must be applied on truncated signals such as each segment is composed of the same number of values. In this particular configuration, if sharp peaks remain at the same amplitude while the number of segments considered in the Welch method increase then these peaks correspond to the modes of the propagating waves inside the gong.

Figure 2 shows Fourier transform of the sound signal of the bigger forcing amplitude. This Fourier transform is computed for 4 different averaging numbers in the conditions discussed before. It demonstrates the presence of wave inside the gong. In fact, numerous sharp peaks remain at a constant amplitude whereas average number increase.

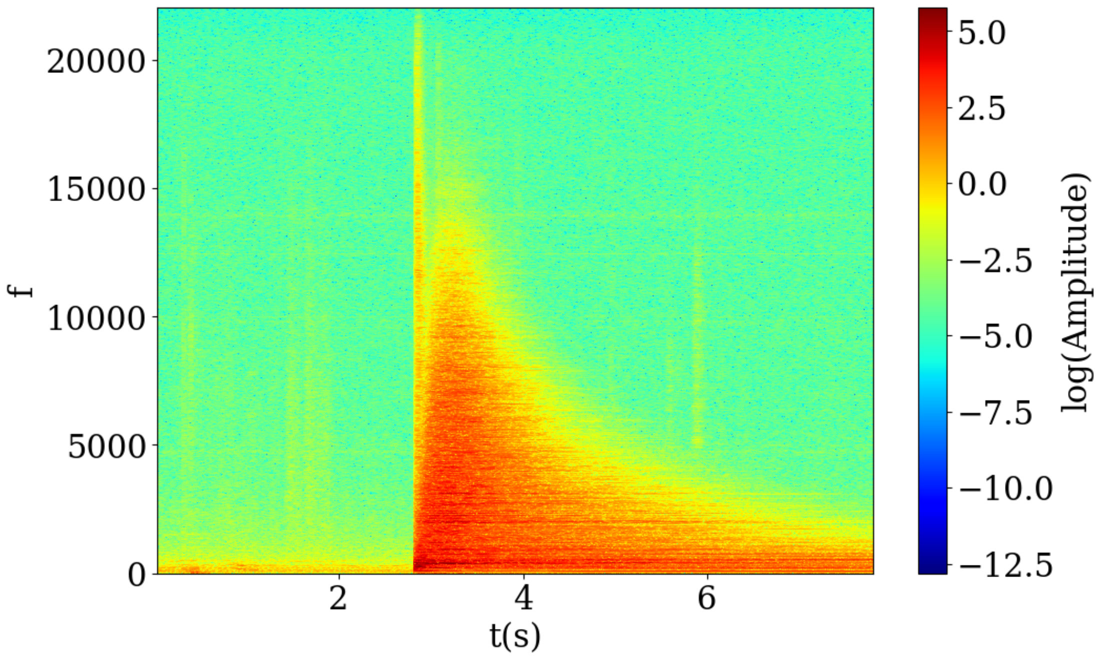

Figure 3: Fourier transform of a freely decrasing configuration of the gong over the time. The gong is strucked around $t = 3$ s.

3.2.2 Transient state

To show that turbulence wave occurs inside the gong, the spectrum of a freely decreasing signal must be computed over the time. Experimentaly, the recording is started before the gong is strucked once and stopped when the song isn't even audible. Fourier transform is then computed on overlapped windows such as for the Welch method. Every Fourier transform is plotted depending on time figure 3. This figure shows four distincts regimes:

- Before the gong is strucked: no signal.
- When the gong is strucked: non pertinent computation. While the discontinuity is inside the computing window the Fourier transform show energy in every frequencies because a discontinuity is formed of all frequencies. The vertical band around $t \sim 3$ s is not a physical energy but just a computational artefact.
- Just after the gong is strucked: the spectrum is developping. At the begining energy is only present at low frequencies but while the time increase the energy begin to be present at higher frequencies. It demonstrate the presence of wave turbulence in the system. In fact, if energy is going from low frequencies to higher frequencies it means a non linear phenomenon is occuring. This second part of the spectrogram is the construction of a turbulent wave cascade.
- A short time after the struck (less than 1 s): the dissipation atenuate the wave turbulence. Dissipation is first acting on high frequencies reducing the amplitude of the signal in these frequencies and then dissipating the whole spectrum.

This study of a transient state of the gong demonstrate presence of wave turbulence inside the gong and show the dynamic of the turbulent cascade.

3.3 Optical measurements

To study more precisely the wave propagation that occur inside the gong, space Fourier transform profilometry is performed on the gong (see §2.3). This type of method allows to measure the local deformation of the gong in a defined surface over the time. A 10kHz camera with 75x85 pixels sensor is used. A surface arround 33x37cm² of the gong is covered by it.

3.3.1 Dispersion relation

The Fourier transform over space and time can be computed on such measurements. If weakly non-linear waves are propagating over the vibrating plate (hypothesis of wave turbulence theory) a thick dispersion relation must apear on the (ω, k) plane.

To check it, Fourier transform is computed over each dimension. Two observations are then possible:

- make a cut in one k direction (for example k_x) and plot the signal energy depending on f and k_x.
- integrate over space angles to compute the signal energy depending on the norm of the wavenumber k.

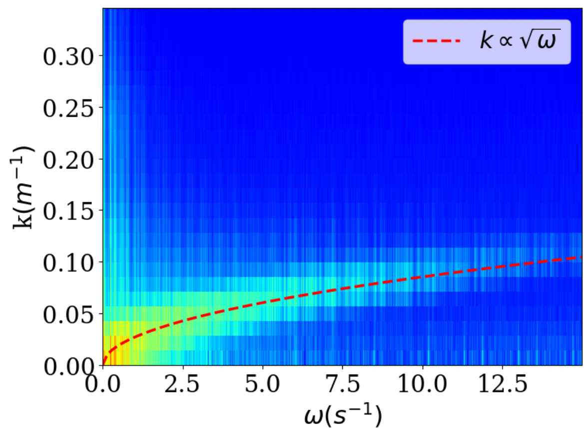

Figure 4: Fourier transform of the velocity of the surface of the gong in the (k,ω) plane.

Figure 4 shows the second observation mentioned. This figure demonstrate an other time the presence of wave propagation in the gong. In fact, in the (ω, k) plane most of the signal energy is condensed arround a curve that can be well fitted with the relation $k \propto \sqrt{\omega}$. This relation can be interpreted as the dispersion relation of the linear waves. The standard deviation of the energy around this fit shows how non linear the waves propagation is. If the propagation was linear, the signal energy would be perfectly localised on the fitting curve and wave turbulence wouldn't apear.

3.3.2 Spatial modes

An other way to visualize such measurements is to compute Fourier transform of the signal over time only. Summing the resulting signal over space allows to determine in which frequencies there is more energy. These peaks correspond to spatial modes of oscillation of circular thin plate (the gong here). Such spatial mode can be expressed with Bessel functions and is parametrized by 2 integers: the number of nodal diameters and the number of nodal circles. Spatial distribution of the energy allong the gong can then be plotted for each frequency peak to visualise these modes.

Figure 5 shows 6 examples of spatial modes of the gong. The first 5 plots show modes with one nodal circle and an increasing number of nodal diameter. The last plot show the mode with two nodal circle and one nodal diameter. Both plot $f_0 = 0.53$ Hz and $f_0 = 0.56$ Hz show modes that must have the same energy so that must oscillate at the same frequency. This removal of degeneracy can be explained by a non perfect geometry of the circular plate. It can also originate from coupling with others modes, especially with non linear interaction.

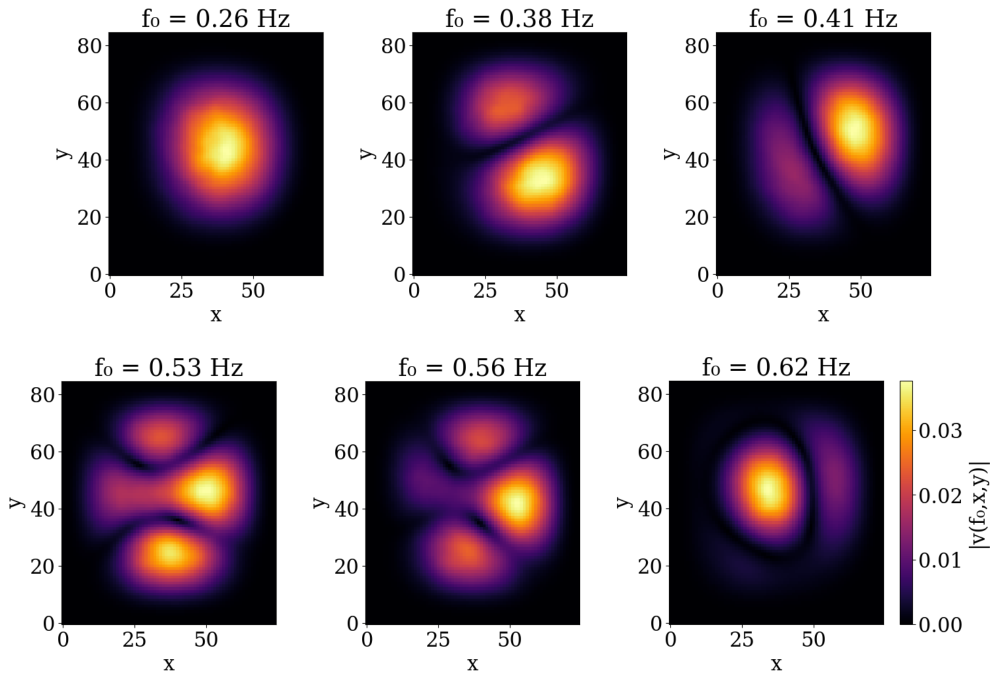

Figure 5: Modes deformation of the circular plate.

3.4 General comments

A circular thin vibrating plate, is a non linear system that can be modelised with perturbation theory. The purely linear model leads to spatial modes defined from Bessel functions and characterized by 2 parameters. The non linear theory leads to turbulence wave theory which is much more difficult to develop.

The gong studied in this experimental work is a good way to observe and confirm linear theory. It's also a nice tool to look at classical concepts of the wave turbulence theory such as wave cascade.

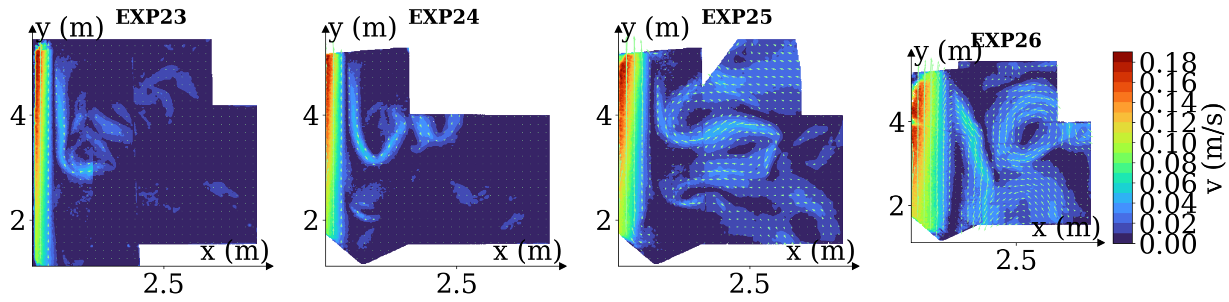

Figure 6: Mean velocity distribution for 4 experiments. The flow rate increase with the experiment number.

4 Coriolis turntable

4.1 Context and experimental setup

Modelising sea currents remain an important topic to understand the global dynamic of water around the world. It gives some important tips for navigation, global warming explanations and shows the complexity of underlying physics. For example, the Gulf Stream current at the east coast of north-America remain a poorly understood phenomenon. Why does this current remain steady with such intensity? Why do this trend is not observed on the western coast of Europe? Harald Sverdrup, Henry Stommel and Walter Munk developped between 1947 and 1950 some models for the ocean to try to explain surface currents. They showed the importance of the earth rotation in the creation of trends. The beta effect is a model that explain quite well sea currents taking into account meridional gradient of Coriolis parameter. Experimentaly, the Coriolis platform allowed to Pierini et.al. [5] to show this beta effect on a rotating flow.

The experimental setup used here is the coriolis platform. A rotating tank is studied, representing the ocean. A forcing flow is performed in a channel linked to the tank. Velocities are measured with PIV method (see §2.4) in an horizontal plane 10 cm bellow the water surface. The goal of the study is to highlight beta effect on this setup. Especially showing that an intense current occur on the "west" coast of the reduced ocean and not on the "east" coast.

4.2 Results

Figure 6 shows mean velocity distributions measured for 4 different pumping flow rate. For each experiment an intense current appear, like expected.

Other measurements are then performed, like visualising Reynolds stress tensor coefficients. These coefficients appear to be maximal in the current zone. Kolmogorov scale is then evaluated to show it is bigger than the PIV spatial resolution. Turbulent dissipation rate is also evaluated like eddy viscosity coefficents.

To conclude these experiments show effects that are in agreement with real observations and Sommel/Munk's theories: an instense western boundary current that shows strong Reynolds stress tensor coefficients takes place in the experience.

5 Turbulent wake in wind tunnel

5.1 Context and experimental setup

Wake instabilities are well studied beceause they appear in a lot of diary situations: every time a solid is moving inside a fluid this type of instability can appear. For example, behind a car, a plane or a submarine. These instabilities can be problematic since they oscillate at a given frequency. This oscillation can put the system in a resonnance that is not expected. Studying wake instabilities is then an issue to prevent resonnance.

This practical work proposes to study the flow arround a cylinder placed inside a laminar tunnel wind. Mean velocity inside the tunnel is measured with a Pitot probe. To study instability behind the obstacle, velocity is measured with a cobra probe that can be moved precisely in the wake of the cylinder.

One can evaluate the Reynold number of such a flow. Considering air viscosity ($\nu = 1.5.10^{-5}\ m.s^{-2}$), mean velocity of the flow ($U \in [5, 10]\ m.s^{-1}$) and diameter of the cylinder ($D = 4$ cm) the Reynolds number reads $Re = \frac{UD}{\nu} \in [1.3, 27].10^3$. In this range of Reynolds numbers von Kármán vorticies are espected in the wake of the cylinder.

The Strouhal number characterize this instability, comparing the characteristic time for advection to the instability's characteristic time. It reads $St = \frac{f_K D}{U}$, where f_K is the frequency of the instability and D and U the diameter and velocity considered for the calculation of the Reynolds number. In the range of Reynolds numbers considered, theory and experimentations shows that the Strouhal number remain constant with a value around $St \sim 0.15$ [1].

5.2 Measurements and results

Several series of measurements are performed varying only one parameter: horizontal position with a fixed height (the one of the cylinder), vertical position at a fixed horizontal point (arround 10 cm behind the obstacle) and velocity of the tunnel wind for fixed position of the probe.

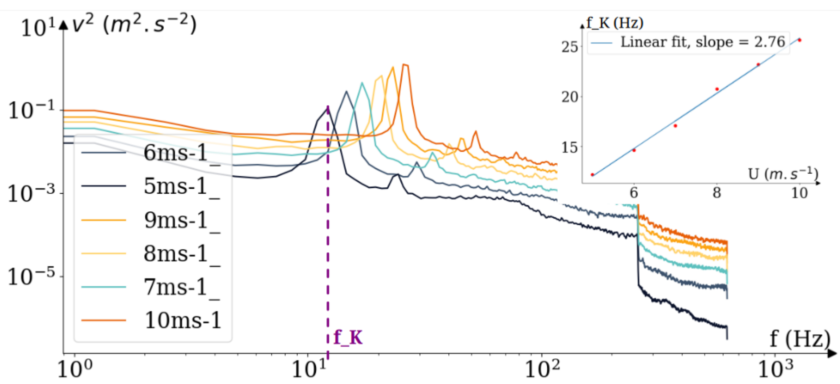

Figure 7: Fourier transform of the velocity behind the cylinder. The Kelvin-Helmoltz frequency f_K increase linearly with velocity (up-right subfigure).

Figure 7 shows Fourier transform (performed with the Welch method, §2.2) for 6 different wind tunnel velocities. First, each spectrum shows a well defined peak between 10 Hz and 100 Hz. This peak is characteristic of von Kármán instability that is espected in such system. The evolution of the von Kármán frequency with flow velocity fit also the theory. In fact, this frequency increase with velocity in the figure 7. Theoricaly, the Strouhal number remains constant so the frequency of the von Kármán instability is proportional to $\frac{U}{D}$. On the top right of the figure 7 a linear fit is performed between f_K and U. It shows a great agreement between fit and data and gives a slope of $\frac{f_K}{U} = 2.76m^{-1}$. Then multilpying by D, the Strouhal number reads $St = 0.11$ wich fit well with the theory mentioned in the previous section.

6 Atmospheric boundary layer

6.1 Context and experimental setup

The atmospheric boundary layer is a part of the atmosphere wich is daily influenced by earth surface. These fluctuations can be explained by an energy balance but some terms are quite hard to determine (like the ground conductivity - see [2]).

The atmospheric boundary layer can be studied with a lot of different types of measurements like wind velocity, temperature, air composition, etc. Such measurements are done in the Ferpeyret clearing under the west face of the Grand Colon near Grenoble. The measurement setup is composed of:

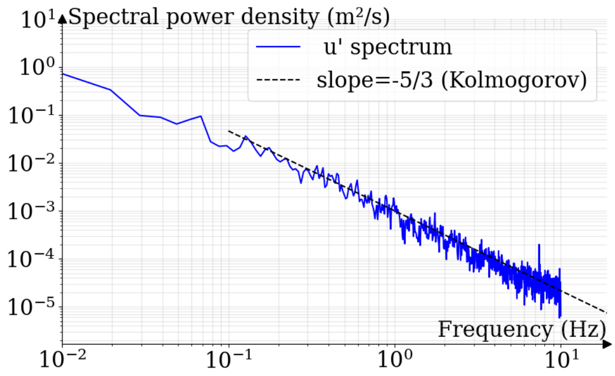

Figure 8: Spectrum of the turbulent velocity calculated from data measured between 2025-11-27 15:30:00 and 2025-11-27 15:35:00.

- 6 Fine Wire Thermocouples (type E) disposed at different altitudes from the ground (from some centimeters to 2 meters);
- 1 infrared temperature sensor that offers a non-contact measuring of the temperature of the ground;
- 1 ultrasonic anemometer for measuring sonic temperature and wind speed in three dimensions;
- 1 digital humidity sensor to measure air composition and to show his impact on the flow.

6.2 Experimental work

Arriving at the station, thermocouples, infrared temperature sensor and ultrasonic anemometer where already disposed on the setup. Every tool is connected to a saving central card and the data is sent with mobile network to a data center. During the experimental work, checks were done to make sure the sensors already present worked well (especially for wind and snow that affected the measurement system). A new sensor has been added to the setup and linked to the central card. The snow chains were then put on to allow the truck to leave the clearing.

6.3 Results

Data measured has been downloaded from the data center. After an important work on the signal to discard parts where sensors where not giving pertinent measurements (NaN) and to chose a day where meteological conditions where adapted to this type of measurements, some study can be done. The first quantity to plot is diurnal variation in temperature that shows periodic oscillations with a 1 day period. General turbulent study can also be performed on velocity measurements showing energy spectrum (fig. 8) or Reynolds tensor coefficients. Plotting vertical distribution of the temperature that increase for the first meter and decrease for higher altitudes.

One can then conclude that the wind measured was in a fully developped turbulence state and the atmospheric boundary layer was about 1 m for the selected data.

7 Conclusion

The four experimentations developped give a wide range of methods to better understand turbulence. In fact, this topic remain an open theorical problem. In this context, every experimental or numerical observation gives important informations about it. The present study gives tools to apprehend theoretical and expermental usual turbulent skills.

Important results of these studies are the following:

- Wave turbulence can be observed in a musical gong performing sound analysis and Fourier transform profilometry. The time evolution of the turbulent cascade is observed on the signal spectrum. The validity of the slightly non linear wave propagation inside the gong is shown.
- The PIV method is used to measure velocity field with a precision under the Kolmogorov scale that gives pertinent analysis of the flow of a reducted model of the Gulf Stream current.
- Turbulent velocity behind a cylinder in a laminar wind tunnel can be measured with a cobra probe. Strouhal number is then calculated to caracterize the von Kármán instability.
- Kolmogorov spectrum is observed on velocity measurements of a montain wind. It is performed in a clearing showing the pertinence of the Kolmogorov (41) theory in such measurements.

A lot of the methods presented here should have been performed for each experiment (for example observing the Kolmogorov spectrum) but the diversity of methods has been favoured in this report. The goal was to highlight the amount of methods learned in this module, whether they are experimental, data analysis or theoretical.

The short time allowed and the lack of a defined framework (except for the gong experiment) made this learning really difficult. A lot of experimental work was based on papers that describe extensive research work. An important time has been spend to define which intersting information can be computed in the given time.

References

[1] C. Brun, S. Aubrun, *et al.* "Coherent Structures and their Frequency Signature in the Separated Shear Layer on the Sides of a Square Cylinder". *Flow Turbulence Combust* 81 (2008), pp. 97–114. DOI: 0.1007/s10494-008-9152-4.

[2] Claudine Charrondière. "Étude in-situ des écoulements catabatiques sur pente alpine forte en situation anticyclonique". French. Thèse de doctorat en météorologie. PhD thesis. Université Grenoble Alpes, 2021.

[3] A. Maurel, P. Cobelli, *et al.* "Experimental and theoretical inspection of the phase-to-height relation in Fourier transform profilometry". *Applied optics* 48 (2009), pp. 380–392. DOI: 0003-6935/09/020380-13$15.00/0.

[4] N. Mordan. "Fourier analysis of wave turbulence in a thin elastic plate". *The European Physical Journal B* 76 (2010), pp. 537–545. DOI: 10.1140/epjb/e2010-00197-y.

[5] Stefano Pierini, Paola de Ruggiero, *et al.* "Laboratory experiments reveal intrinsic self-sustained oscillations in ocean relevant rotating fluid flows". *Scientific reports* 12 (2022). DOI: 10.1038/s41598-022-05094-1.